Supporting Information for:

Highly-dispersed and disordered nickel-iron layered hydroxides and sulphides: robust and high-activity water oxidation catalysts

Manjunath Chatti,[ab] Alexey M. Glushenkov,[c] Thomas Gengenbach,[d] Gregory P. Knowles,[a] Tiago C. Mendes,[a] Amanda V. Ellis,[c] Leone Spiccia,[ab] Rosalie K. Hocking,[e] and Alexandr N. Simonov*[ab]

[a]School of Chemistry and the [b]ARC Centre of Excellence for Electromaterials Science, Monash University, Victoria, 3800, Australia

[c]Department of Chemical Engineering, The University of Melbourne, Parkville, Victoria 3010, Australia

[d]Commonwealth Scientific and Industrial Research Organisation Manufacturing, Clayton, Victoria 3168, Australia

[e]Department of Chemistry and Biotechnology, Swinburne University of Technology, Victoria, 3122, Australia

TABLE OF CONTENTS

Table S1. Activity of selected transition metal based catalysts for water electrooxidation in 1 M KOH. [a]

Catalyst (loading / mg cm^{-2}, electrode)	Synthesis method	A_{BET} / m^2 g^{-1}	η_{10} [b] /V	i_{cat} [c] / A g^{-1}		j_{BET} [c] / mA cm^{-2}		Ref.
				0.25 V	0.30 V	0.25 V	0.30 V	
$Fe_6Ni_{10}O_x$ (0.1, GC [d])	Aerosol-spraying	n.a. [e]	0.286	24	150	n.a.	n.a.	S1
Ni_3FeN (0.35, GC)	Microemulsion and thermal ammonolysis	n.a.	0.280	28	57	n.a.	n.a.	S2
Gelled-FeCoW (0.21, GC)	Ageing and Annealing	94	0.223	129	n.a.	0.14	*n.a.*	S3
$Co_{0.85}Se/Ni_{0.9}Fe_{0.1}$ (4, G_{foam} [f])	Multistep hydrothermal	156	0.150	20	60	0.01	0.04	S4
RuO_2 (0.05, GC)	Multistep thermal decomposition	120	470	7	10	0.006	0.008	S5
IrO_2 (0.05, GC)	Multistep thermal decomposition	71	450	4	8	0.006	0.011	S5

[a] All data were reported corrected for ohmic losses. [b] Overpotential required to achieve 10 mA cm$^{-2}_{geom.}$ (normalised to the geometric surface area); derived from quasi-steady-state Tafel plot data (if available) or voltammograms. [c] Current density normalised to the catalyst mass (i) or BET surface area (j) at η = 0.25 and 0.30 V. [d] Glassy carbon. [e] Not available. [f] Graphene foam.

SUPPLEMENTARY REFERENCES

S1. L. Kuai, J. Geng, C. Chen, E. Kan, Y. Liu, Q. Wang and B. Geng, *Angew. Chem. Int. Ed.*, 2014, **126**, 7677-7681.

S2. X. Jia, Y. Zhao, G. Chen, L. Shang, R. Shi, X. Kang, G. I. N. Waterhouse, L.-Z. Wu, C.-H. Tung and T. Zhang, *Adv. Energy Mater.*, 2016, **6**, 1502585-n/a.

S3. B. Zhang, X. Zheng, O. Voznyy, R. Comin, M. Bajdich, M. García-Melchor, L. Han, J. Xu, M. Liu, L. Zheng, F. P. García de Arquer, C. T. Dinh, F. Fan, M. Yuan, E. Yassitepe, N. Chen, T. Regier, P. Liu, Y. Li, P. De Luna, A. Janmohamed, H. L. Xin, H. Yang, A. Vojvodic and E. H. Sargent, *Science*, 2016, **352**, 333-337.

S4. Y. Hou, M. R. Lohe, J. Zhang, S. Liu, X. Zhuang and X. Feng, *Energy Environ. Sci.*,, 2016, **9**, 478-483.

S5. Y. Lee, J. Suntivich, K. J. May, E. E. Perry and Y. Shao-Horn, *J. Phys. Chem. Lett.*, 2012, **3**, 399-404.

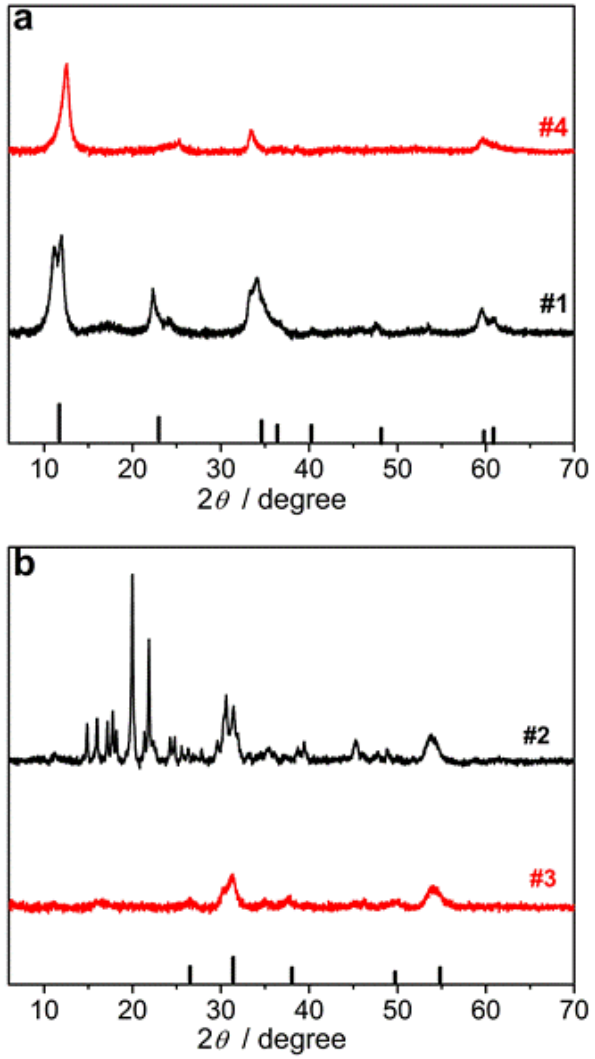

Figure S1. X-ray diffraction patterns of (a) $Ni_{0.9}Fe_{0.1}$ hydroxides and (b) materials obtained during sulphidation of these hydroxides following the procedures #1-4 summarised in Table S2. Vertical lines show the tabulated positions and relative intensities for (a) $Ni_{0.9}Fe_{0.1}$ LDH (JCPDS# 38-0715) and (b) $Ni_{0.75}Fe_{0.25}S_2$ (PDF#11-0099).

Table S2. Conditions explored herein for the synthesis of nickel-iron layered double hydroxides and sulphides.

#	Material	Synthesis Method	Precursors	Reaction parameters			Layer stability
				Temperature / °C	Time	Solvent	
1[a]	$Ni_{0.9}Fe_{0.1}$ LDH	Hydrothermal	$NiCl_2$, $Fe(NO_3)_3$ Urea Trisodium citrate	150	24 h	Water	Stable
2[a]	$Ni_{0.9}Fe_{0.1}$ sulphide	Solvothermal	$Ni_{0.9}Fe_{0.1}$ LDH **#1** Thioacetamide	120	6 h	Ethanol	**Sulphides not formed**
3	$Ni_{0.9}Fe_{0.1}$ sulphide	Microwave	NiFe LDHs **#1** Thioacetamide	150	0.5 h	Ethanol	Unstable
4	$Ni_{0.9}Fe_{0.1}$ LDH	Microwave	$NiCl_2$, $Fe(NO_3)_3$ Urea Trisodium citrate	180	1 h	Water	Unstable
5	$Ni_{0.9}Fe_{0.1}$ sulphide	Microwave	NiFe LDH **#4** Thioacetamide	120-180	0.5 h	Ethanol	Unstable
6	$Ni(OH)_2$	Microwave	$Ni(CH_3COO)_2$ Urea	120	1 h	Water	Stable
7	NiS_2	Microwave	$Ni(OH)_2$ **#6** Thioacetamide	150	0.5 h	Ethanol	Stable
8	$Ni_{0.75}Fe_{0.25}$ LDH	Microwave	$Ni(CH_3COO)_2$ $Fe(NO_3)_3$ Urea	120 °C	1 h	Water	Stable
9	$Ni_{0.75}Fe_{0.25}$ sulphide	Microwave	NiFe-LDH **#8** Thioacetamide	120-180 °C	0.5 h	Ethanol	Stable

[a] Synthesis procedure as in Long *et al. J. Am. Chem. Soc.* **2015,** 137, 11900−11903**.**

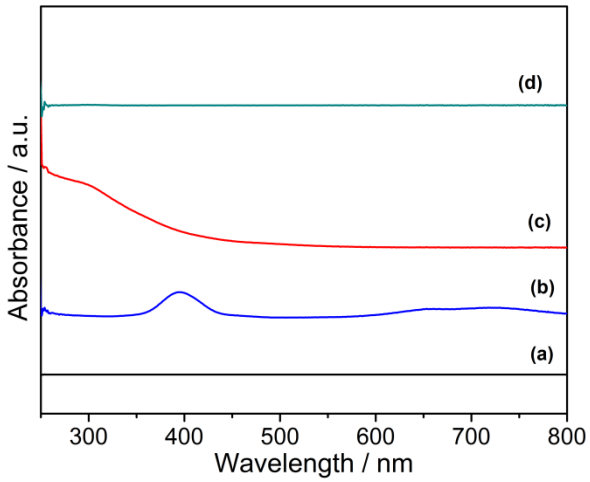

Figure S2. UV-Vis absorption spectra of (a) Milli-Q-purified water, (b) 75 mM $Ni(CH_3COO)_2$ in H_2O, (c) 25 mM $Fe(NO_3)_3$ in H_2O, and (d) supernatant solution after microwave synthesis of $Ni_{0.75}Fe_{0.25}(OH)_{2+x}$.

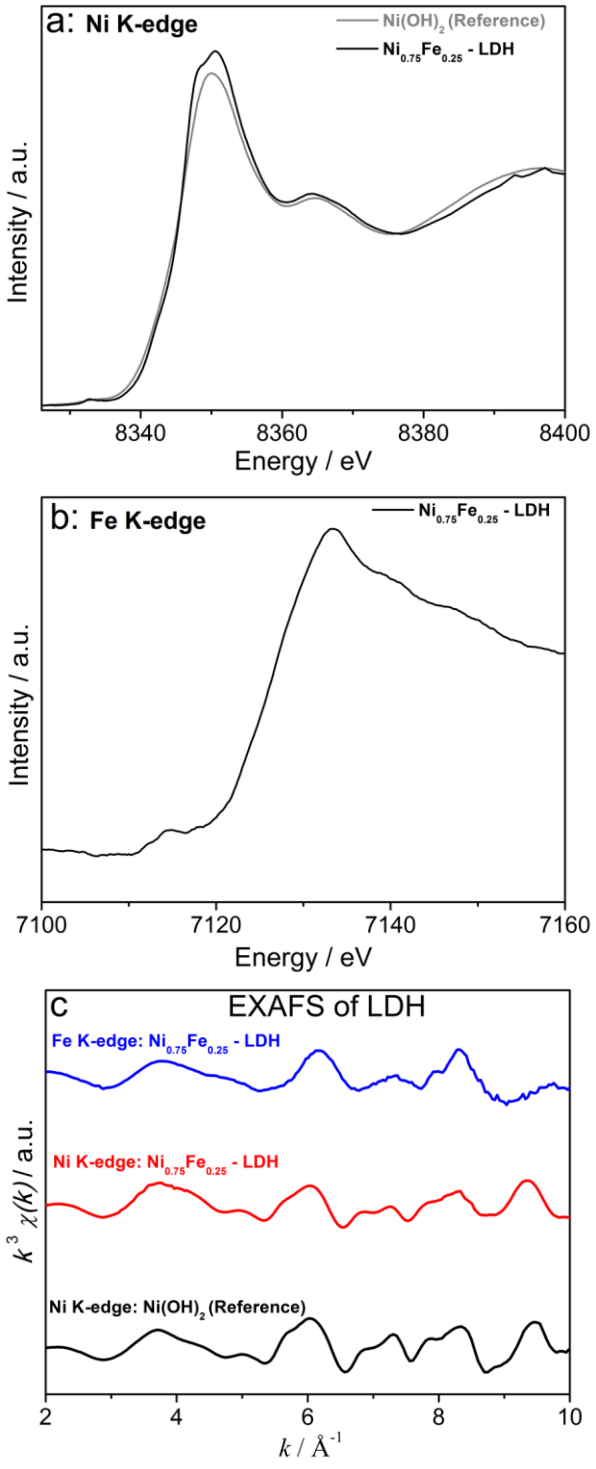

Figure S3. XAS characterisation of $Ni_{0.75}Fe_{0.25}(OH)_{2+x}$: (a) Ni K-edge XANES, (b) Fe K-edge XANES, (c) Fe (*blue*) and Ni (*red*) K-edge EXAFS. *Grey* traces show spectra for the $Ni(OH)_2$ reference material.

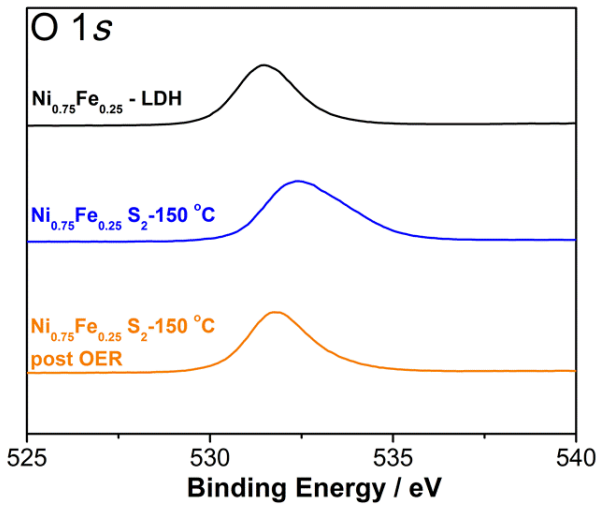

Figure S4. High-resolution O 1s spectra for microwave-synthesised $Ni_{0.75}Fe_{0.25}(OH)_{2+x}$ (*black*) and $Ni_{0.75}Fe_{0.25}S_2$ (synthesised at 150°C) that was freshly prepared (*blue*) or used to catalyse the OER at 10 mA $cm^{-2}_{geom.}$ for 12 h at 25 °C (*orange*).

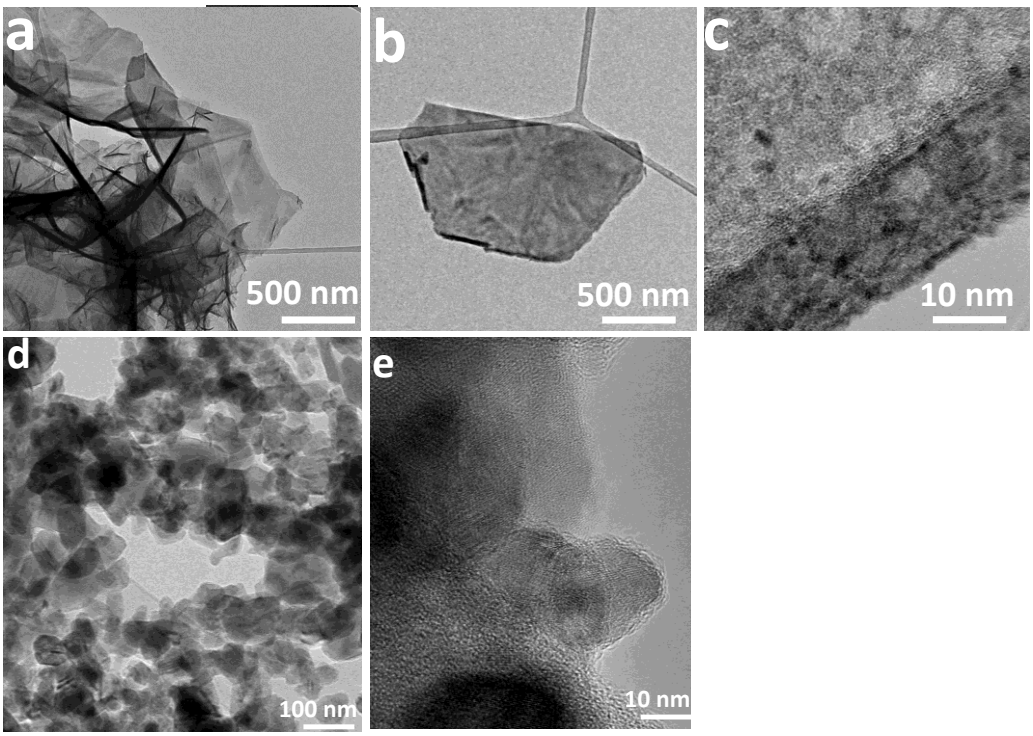

Figure S5. TEM images of microwave-synthesised (a-c) *α*-$Ni(OH)_2$ and (d-e) NiS_2.

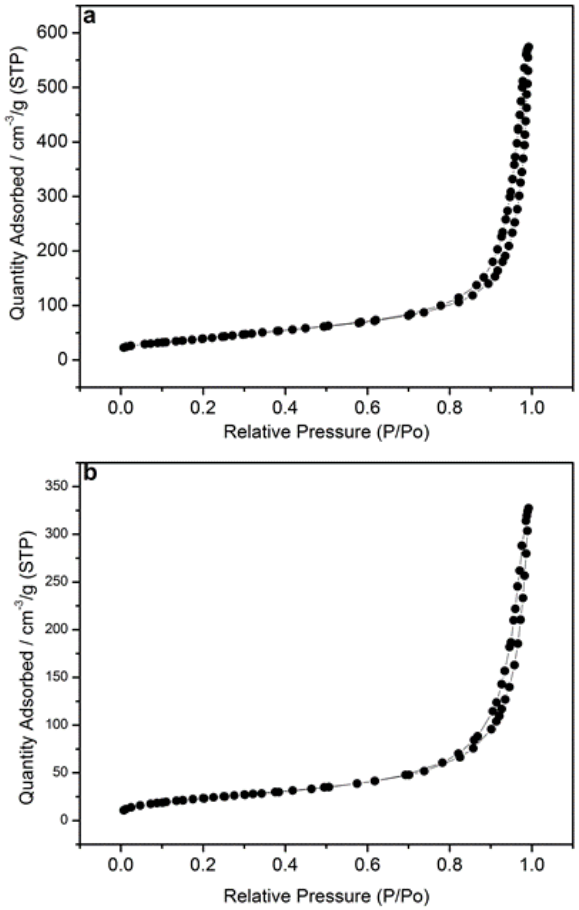

Figure S6. N_2 adsorption-desorption isotherms of microwave-synthesised (a) $Ni_{0.75}Fe_{0.25}(OH)_{2+x}$ and (b) $Ni_{0.75}Fe_{0.25}S_{2+y}$ (obtained at 150°C).

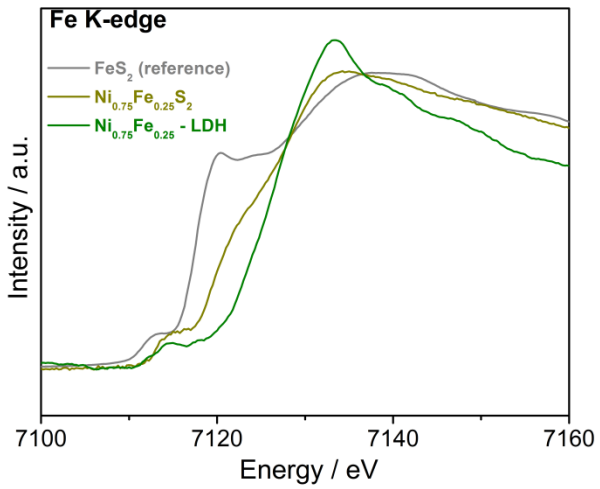

Figure S7. Fe K-edge XANES spectra of microwave-synthesized $Ni_{0.75}Fe_{0.25}(OH)_{2+x}$ (*green*) and $Ni_{0.75}Fe_{0.25}S_{2+y}$ (obtained at 150 °C) (*tan*). *Grey* trace shows spectra for the FeS_2 reference.

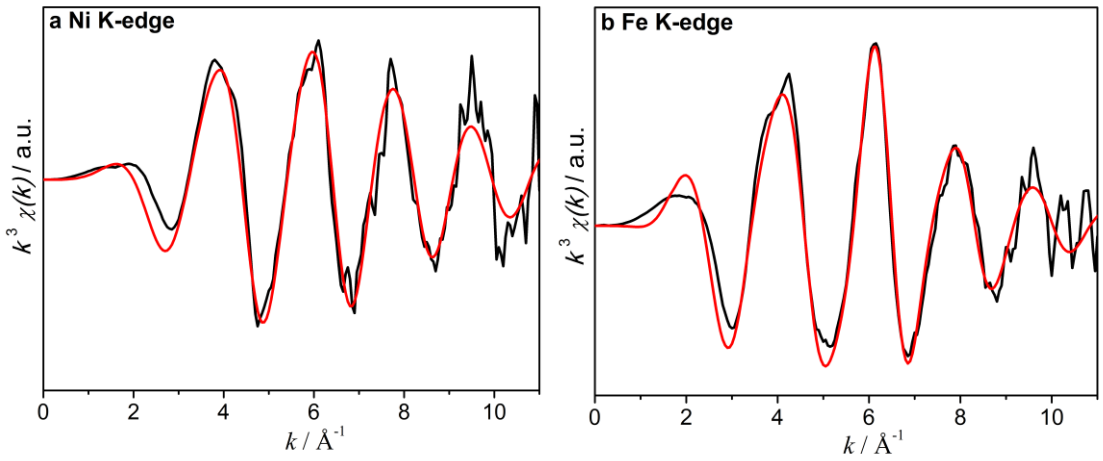

Figure S8. Comparison of experimental (*black*) and simulated (*red*) EXAFS data for microwave-synthesised $Ni_{0.75}Fe_{0.25}S_{2+y}$ (150 °C): (a) Ni K-edge; (b) Fe K-edge. Simulations are based on pyrite structure and parameters in Table S3.

Table S3. Parameters used in EXAFS simulations shown in Figure S8.

	N^a	S02 ^{b}	σ^2 / Å$^{2\,c}$	E0 / eV	R / Å ^{e}	Re (crystal str) / Å ^{f}
Fe-S	6	0.673	0.01428	-14.495	2.216	2.39
Fe-S (2)	6	0.673	0.02647	-14.495	3.1417	3.52
Fe-Ni	12	0.673	0.02903	-14.495	3.859	4.00
Reduced chi-square: 392.67 R-factor 0.003						
Ni-S	6	1.27	0.01104	-21.097	2.211	2.39
Ni-S (2)	6	1.27	0.04664	-21.097	3.0513	3.52
Ni-Ni	12	1.27	0.0312	-21.097	3.790	4.00
Reduced chi-square 248.63 R-factor 0.008						

[a] Coordination number; [b] Amplitude reduction parameter; [c] Debye-Waller parameter; [d] Binding energy; [e] Interatomic distance; [f] Distance from the crystal structure data.

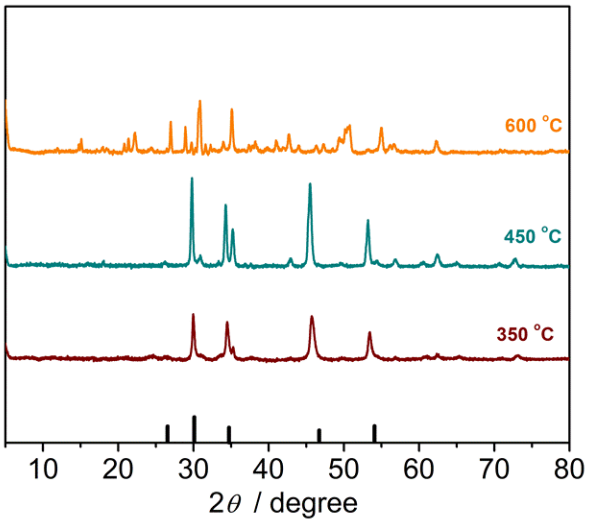

Figure S9. XRD patterns of $Ni_{0.75}Fe_{0.25}S_2$ (150°C) after annealing in N_2 atmosphere at different temperatures: 350 (*wine*), 450 (*cyan*), and 600 °C (*orange*).

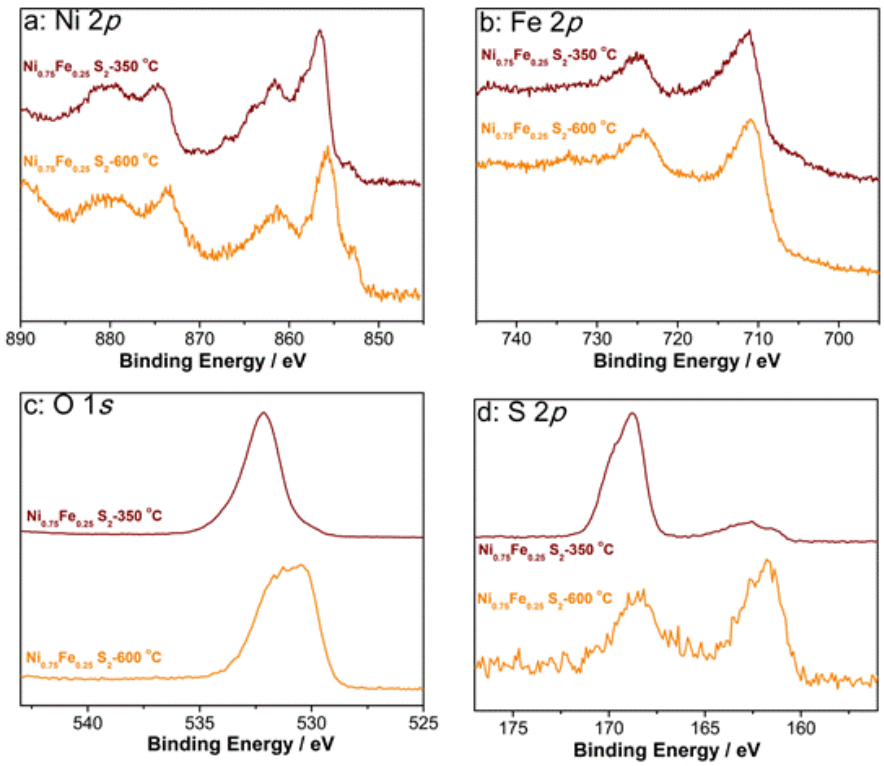

Figure S10. High-resolution (a) Ni 2p, (b) Fe 2p, (c) O 1s, and (d) S 2p spectra for $Ni_{0.75}Fe_{0.25}S_{2+y}$ (synthesised at 150°C) and annealed at 350 (*wine*) and 600 °C (*orange*).

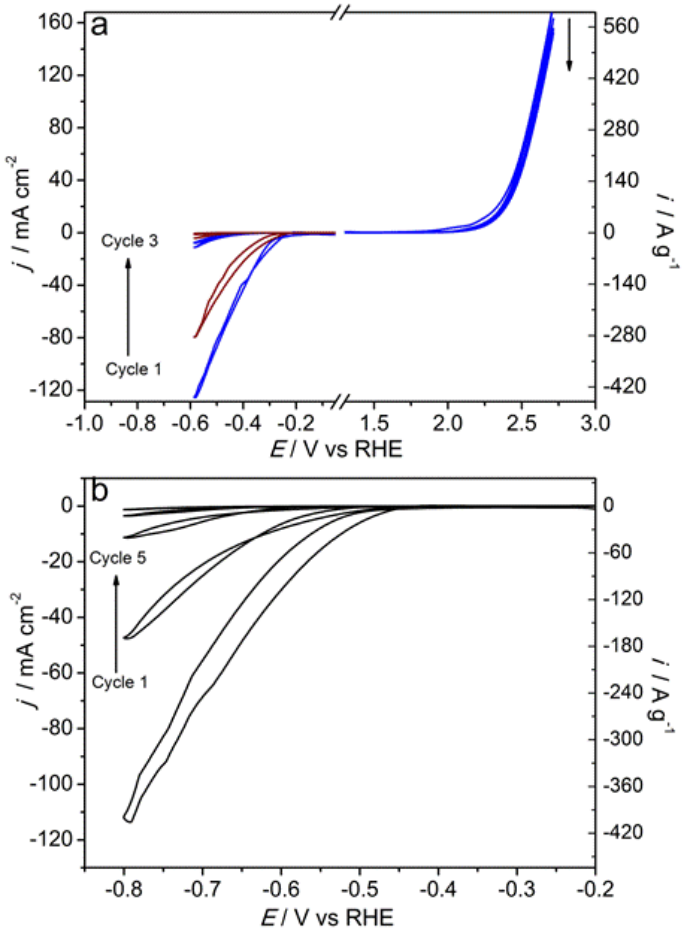

Figure S11. Electrocatalytic activity of the microwave-synthesised (150 °C) materials in stirred aqueous 0.5 M H_2SO_4: (a) HER and OER voltammetric profiles for as-synthesised $Ni_{0.75}Fe_{0.25}S_{2+y}$ (*blue*), and $Ni_{0.75}Fe_{0.25}S_{2+y}$ annealed at 350 °C in the N_2 atmosphere (*wine*); (b) HER voltammetric profile for NiS_2. Data for the HER and OER were obtained in N_2- and air-saturated solutions, respectively. Currents are normalised to the geometric surface area of the electrodes and mass of the catalysts. Catalyst loading was 0.28 mg cm^{-2}.

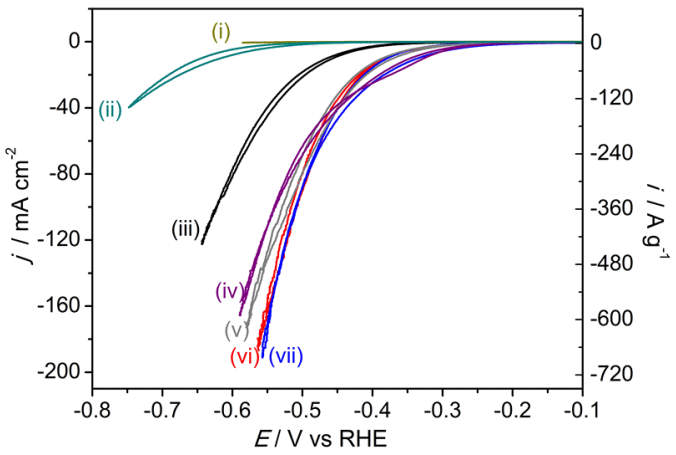

Figure S12. Cyclic voltammograms (scan rate 0.005 V s^{-1}) for reduction of stirred aqueous 1 M KOH using a glassy carbon electrode that was (i) unmodified, or coated with 0.28 mg cm^{-2} of microwave-synthesised (ii) α-$Ni(OH)_2$, (iii) $Ni_{0.75}Fe_{0.25}(OH)_{2+x}$, (iv) NiS_2 or $Ni_{0.75}Fe_{0.25}S_2$ produced at (v) 120, (vi) 180 or (vii) 150 °C. Data were post-corrected for the iR_u drop (R_u = 15-18 Ω).

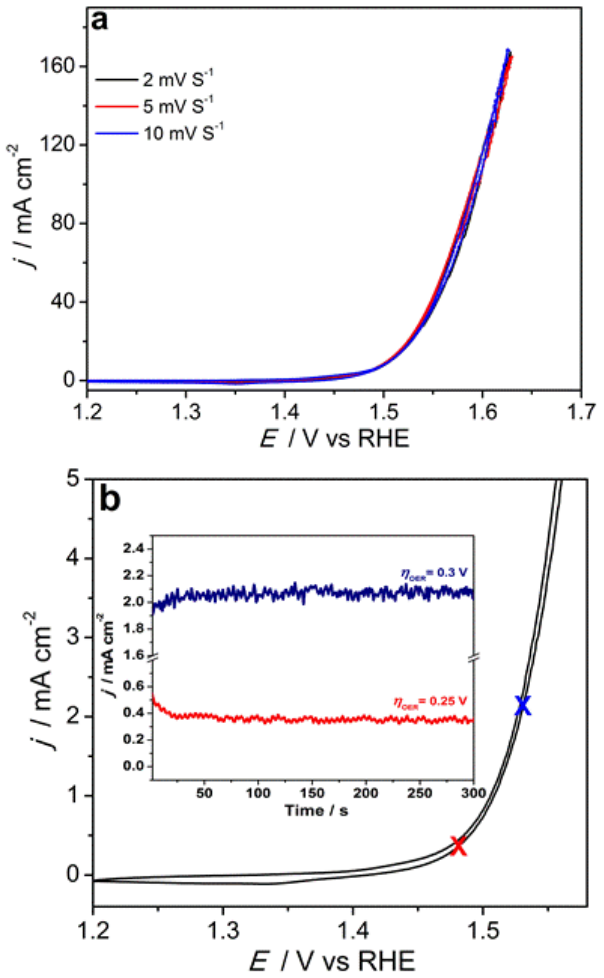

Figure S13. Electrooxidation of stirred aqueous 1 M KOH using a glassy carbon electrode functionalised with microwave-synthesised $Ni_{0.75}Fe_{0.25}S_{2+y}$ (obtained at 150°C): (a) effect of scan rate (*black* - 0.002 V s^{-1}; *red* - 0.005 V s^{-1}; *blue* - 0.010 V s^{-1}) on cyclic voltammograms for catalyst loading 0.28 mg cm^{-2} (data were post-corrected for the IR_u drop; R_u = 15 Ω); (b) comparison of cyclic voltammogram (scan rate 0.005 V s^{-1}) with quasi-steady-state current densities derived from chronoamperograms recorded at 0.25 (×) and 0.30 V (×) OER overpotential for catalyst loading 0.03 mg cm^{-2} (*j*-*t* transients are shown in the inset).

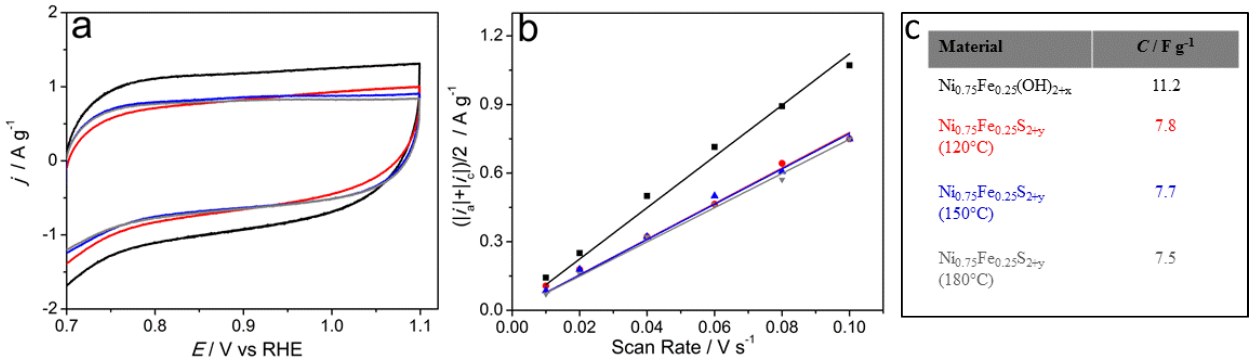

Material	*C* / F g^{-1}
$Ni_{0.75}Fe_{0.25}(OH)_{2+x}$	11.2
$Ni_{0.75}Fe_{0.25}S_{2+y}$ (120°C)	7.8
$Ni_{0.75}Fe_{0.25}S_{2+y}$ (150°C)	7.7
$Ni_{0.75}Fe_{0.25}S_{2+y}$ (180°C)	7.5

Figure S14. (a) Cyclic voltammograms (scan rate 0.100 V s^{-1}) of microwave-synthesised $Ni_{0.75}Fe_{0.25}(OH)_{2+x}$ (*black*) and $Ni_{0.75}Fe_{0.25}S_{2+y}$ (obtained at 120 (*red*), 150 (*blue*) and 180 °C (*grey*)) within the potential range devoid of significant faradaic processes. Catalysts were immobilised on a glassy-carbon electrode at Γ = 0.28 mg cm^{-2}. Electrolyte solution: quiescent aqueous 1 M KOH. Currents are normalised to the catalyst mass. (b) Dependence of the simple average of the anodic and cathodic current densities at 0.9 V *vs.* RHE derived from cyclic voltammograms as those exemplified in panel **a** on a potential scan rate. Solid lines are linear fits to the experimental data. (c) Specific capacitance derived from the data in panel **b**.

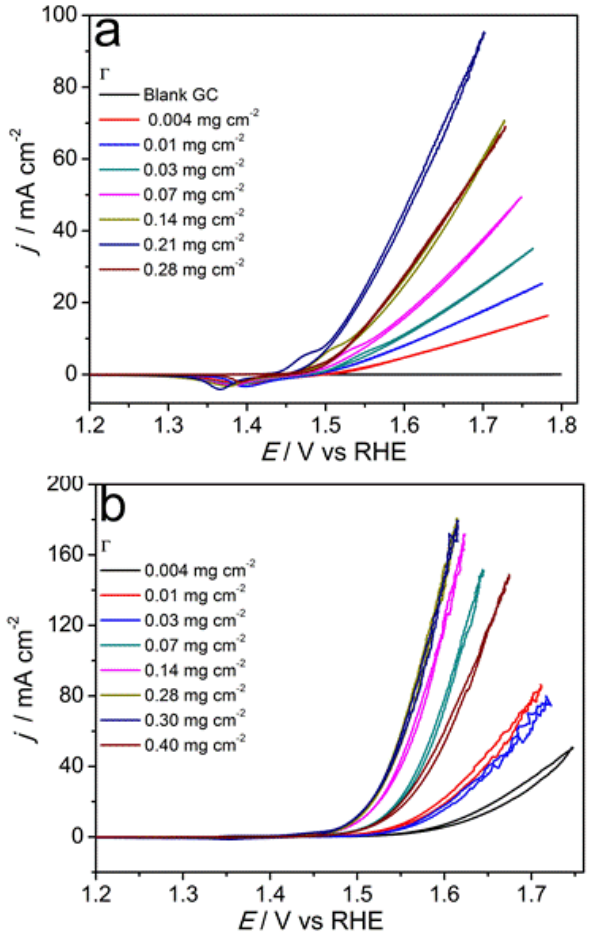

Figure S15. Effects of catalyst loading (Γ) on cyclic voltammograms (scan rate 0.005 V s^{-1}) obtained for glassy-carbon electrodes functionalised with microwave-synthesised (a) $Ni_{0.75}Fe_{0.25}(OH)_{2+x}$ and (b) $Ni_{0.75}Fe_{0.25}S_{2+y}$ (synthesis temperature 150°C) in contact with stirred aqueous 1 M KOH. Currents are normalised to the geometric surface area of the electrode. Data were post-corrected for the IR_u-drop (R_u = 13-15 Ω).

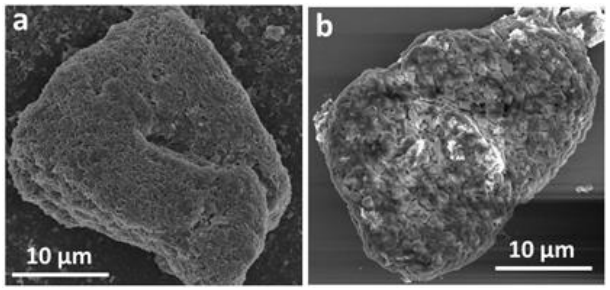

Figure S16. SEM images of microwave-synthesised (a) $Ni_{0.75}Fe_{0.25}(OH)_{2+x}$ and (b) $Ni_{0.75}Fe_{0.25}S_{2+y}$ (obtained at 150°C). Samples were drop-cast on a flat silicon support.

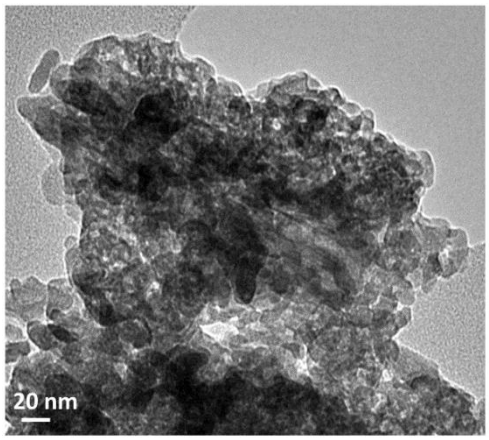

Figure S17. TEM image of the $Ni_{0.75}Fe_{0.25}S_{2+y}$ material synthesised under microwave conditions at 150 °C that was used as an electrocatalyst for electrooxidation of stirred aqueous 1 M KOH for 12 h at 1.5 V *vs.* RHE at 25 °C (chronoamperogram shown in Figure 7a of the main text).

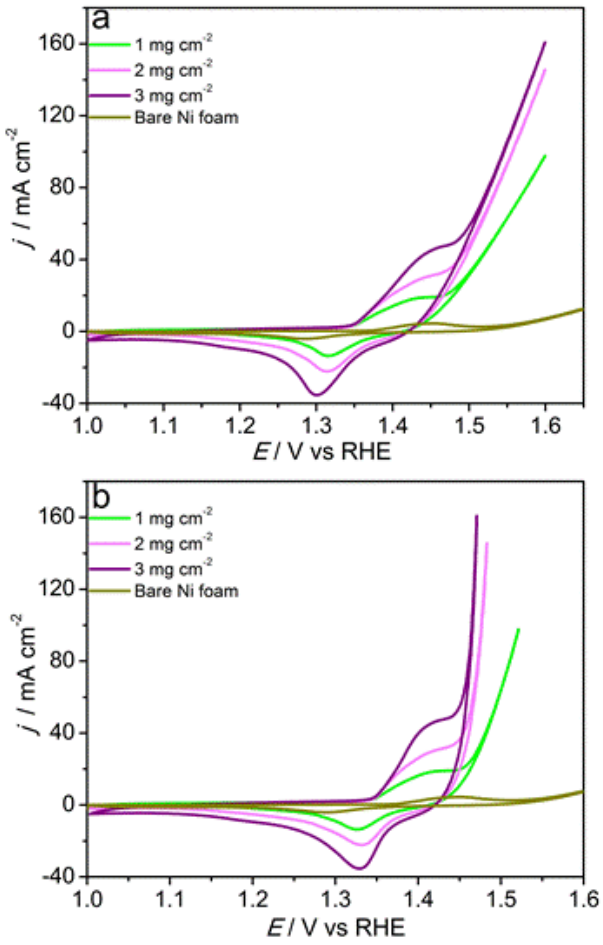

Figure S18. Cyclic voltammograms (scan rate 0.005 V s^{-1}) for oxidation of stirred 1 M KOH with a nickel foam electrode that was unmodified (*tan*), or coated with 1.0 (*light green*), 2.0 (*pink*) or 3.0 mg cm^{-2} (*purple*) of $Ni_{0.75}Fe_{0.25}S_{2+y}$ synthesised using a microwave method at 150 °C. Panel (a) shows raw experimental data normalised to the geometric surface area of the electrode, and panel (b) shows data that were post-corrected for iR_u-drop (R_u = 0.5 Ω).

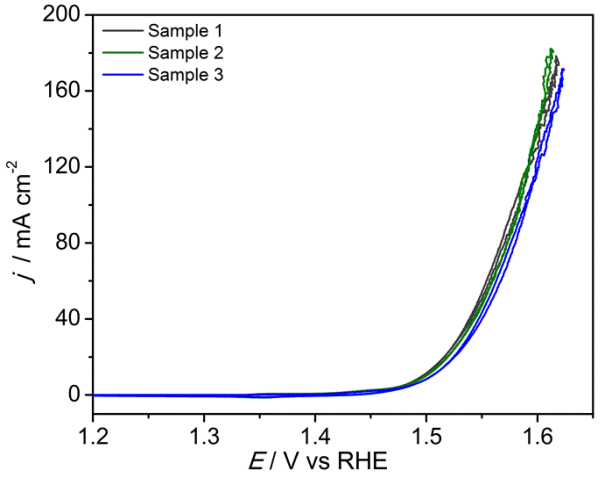

Figure S19. Cyclic voltammograms (scan rate 0.005 V s^{-1}) for oxidation of stirred 1 M KOH catalysed by three independent samples of $Ni_{0.75}Fe_{0.25}S_{2+y}$ each synthesised using a microwave method at 150 °C. Catalysts were immobilised on a glassy-carbon electrode at $\Gamma = 0.28$ mg cm^{-2}. Currents are normalised to the geometric area of the electrode. Data were post-corrected for iR_u losses (R_u = 13-15 Ω).